



Rockburst mechanism and the law of energy accumulation and release in mining roadway: a case study

Feng Du^{1,2} · Ji Ma^{2,3} · Xiaofei Guo¹ · Tianfeng Wang¹ · Xiaohang Dong³ · Jiashuo Li³ · Shulei He¹ · Dilinaer Nuerjuma¹

Received: 1 December 2021 / Accepted: 16 June 2022
© The Author(s) 2022

Abstract

The rockburst dynamic disasters in the process of deep coal mining become more and more serious. Taking the rockburst occurred in the 23130 working face of Yuejin Coal Mine as the engineering background, we study the characteristics of mining stress field around roadway, the plastic failure morphological characteristics of surrounding rock and the accumulation/release law of elastic energy before and after burst. An analysis model quantitatively describing the physical process of rockburst in the mining roadway is established, and the calculation method of dynamic release of elastic energy in the physical process of rockburst is deduced. The mechanism of rockburst in mining roadway is revealed. The results show that an “L-shaped” stress concentration zone is formed within 100 m of the 23130 working face, and the principal stress ratio of the surrounding rock of the transportation roadway is 2.59–4.26. The change of the direction of the maximum principal stress has a significant effect on the burst appearance characteristics. The failure strength of different sections of the mining roadway is characterized by the elastic energy release value. With the increase of the working face distance, the elastic energy released by burst failure and the expansion variation of failure boundary radius show a nonlinear variation law that tends to decrease steadily after sharp fluctuation. The closer to the working face, the higher the burst risk. At a distance of 10 m from the working surface, the maximum principal stress reaches its maximum value. The butterfly-shaped failure system generated by the surrounding rock of the roadway has energy self-sustainability, and the elastic energy released by the sudden expansion of the butterfly leaf is enough to cause a burst damage of 1.9 magnitude. This work could provide theoretical support for the prediction and prevention of rockburst.

Keywords Coal · Rockburst · Mining roadway · Plastic failure · Dynamic and static load · Elastic energy

1 Introduction

Safe, green and efficient mining is an important way to optimize the development of coal resources, maximize economic and social benefits and minimize ecological effect (Fan et al. 2017; Li 2021; Yuan 2016). However, in recent

years, with the gradual deep mining of coal mines, coal and rock dynamic disasters have become more and more serious (Du et al. 2020; Li et al. 2016, 2021; Si et al. 2021). Rockburst is one of the most serious dynamic disasters, which seriously restricts the safe and efficient production of coal (Du and Wang 2019; Li et al. 2017; Yardimci and Karakus 2020; Zhou et al. 2018). In recent years, with the development of deep mining, the continuous increase of mining depth and mining area lead to the increasing complexity of coal mining conditions, which also aggravates the occurrence of rockburst (Konicek and Waclawik 2018; Li et al. 2018; Wang and Du 2020; Xue et al. 2020; Zhang et al. 2017).

The mechanism of rockburst is a hot topic and scientific problem for a long time. The research on the mechanism of rockburst is essentially to find out the causes, inducing factors and dynamic mechanical process of rockburst, which is the premise and basis for realizing rockburst monitoring,

✉ Ji Ma
showsma@hpu.edu.cn

¹ Beijing Key Laboratory for Precise Mining of Intergrown Energy and Resources, China University of Mining and Technology (Beijing), 100083 Beijing, China

² State and Local Joint Engineering Laboratory for Gas Drainage & Ground Control of Deep Mines, Henan Polytechnic University, 454003 Jiaozuo, Henan, China

³ School of Safety Science and Engineering, Henan Polytechnic University, 454003 Jiaozuo, Henan, China

early warning and effective prevention and control. The early classical rockburst theories include strength theory, stiffness theory, energy theory and burst tendency theory (Bieniawski et al. 1969; He et al. 2021; Wang et al. 2019). Later, Zhang (1987) put forward the deformation system instability theory of rockburst, and derived the standard criterion of rockburst from the perspective of coal rock deformation and failure process using Function theory. Qi et al. (2013) put forward the stress control theory and deduced the expression of unit stress gradient which can be used to evaluate the burst risk and burst risk area. Pan (2018) presented the instability theory of rockburst disturbance response, and defined the expression of critical stress expression when rockburst occurs. Focusing on the changes of stress before and after rockburst and the morphological characteristics of plastic failure of coal rock system, some scholars constructed the analysis model of occurrence mechanism of butterfly rockburst in roadway, and put forward the judgment criterion of butterfly rockburst (Ma et al. 2016; Zhao et al. 2013).

These research results forming the theoretical system play a very important role in qualitatively expounding and revealing the mechanism of rockburst. However, we still could not achieve accurate prediction, real-time monitoring and effective prevention and control of rockburst. The reason is that it is difficult to explain all rockburst phenomena with unified theory and relatively simple mathematical expressions. In particular, the complex coal seam occurrence conditions, coal seam mining conditions, geological tectonic movement in the deep underground, as well as various disturbance factors such as blasting operation, roof fracture and mining disturbance in the process of stope mining will have a significant influence on the occurrence of rockburst (Chen 2020; Dai et al. 2021; Jiang et al. 2014; Zhu et al. 2018). Therefore, a number of research based on the mechanism of rockburst under specific conditions have emerged. For example, He et al. (2021) studied the mechanism of rockburst during mining of extremely inclined extra thick coal seam. studied the mechanism of rockburst induced by complex geological structure areas such as faults. Jiang et al. (2020) analyzed the potential burst of seismic moment released by fault tectonic activity on rockburst in the mining process of longwall face intersecting with fault. Zhao et al. (2020) studied the burst instability mechanism of adjacent goaf roadway in deep mining in Xinjie mining area. Qi et al. (2019) studied the occurrence mechanism of mine group rockburst in the mining process of adjacent working faces between adjacent mines under the conditions of F16 fault and huge thick gravel roof in Yima mining area. Rockburst is essentially the mechanical behavior of in-situ coal and rock mass in slow or sudden stress field. The coupling action of mining stress field, energy field, plastic failure mode of surrounding rock in mining area and inducing factors is very

important for the appearance of burst mechanical behavior of coal and rock mass. However, there are few reports on the coupling quantitative variation characteristics of the above four parameters in the evolution process of rockburst in mining roadway.

Therefore, in this work, taking the rockburst case in the Yuejin Coal Mine in Yima mining area as the research object, we systematically study the distribution law of mining stress field, the evolution law of plastic failure characteristics of surrounding rock of mining roadway, and the law of energy accumulation and release of surrounding rock. We also establish a physical analysis model for quantitatively describing the occurrence process of rockburst in mining roadway, and reveals the occurrence mechanism of rockburst in mining roadway, which could certainly provide theoretical support for the prediction and prevention of rockburst.

2 Overview of rockburst accidents in Yuejin Coal Mine

2.1 Geological overview of 23130 working face in Yuejin Coal Mine

The 23130 working face is located in the east flank of Yuejin Coal Mine. The mine excavation engineering plan is shown in Fig. 1. The protective coal pillar at the mine field boundary of Yuejin Changcun is in the east side. The downhill protective coal pillar in mining area 23 is in the west side. The 23110 fully mechanized mining face (mined) is in the north side, and the 23150 fully mechanized top coal caving face (not mined yet) is in the south side. The average burial depth of 23130 working face is 830 m, and the strike direction is 1124 m long. The recoverable length is 1002 m, and the working face inclination width is 185 m. In addition, the thickness of the coal seam is 6.6–9.2 m, and the inclination angle is 10°–16°. The mining method is fully mechanized top coal caving with long wall retreating, full height mining at one time, and natural caving method is used to control the roof.

2.2 Structure characteristics and strength test of surrounding rock

At a position 650 m from the stop line in the 23130 working face of Yuejin Coal Mine, there are the detection results of the roof surrounding rocks structure in the belt transport roadway, as shown in Fig. 2a. It can be seen from Fig. 2a that the roof is mainly gray-black mudstone with a thickness of more than 21.4 m, which is in a more complete state but fewer free layers. Among them, the size between 20 and

Fig. 1 Layout of the working face in Yuejin Coal Mine

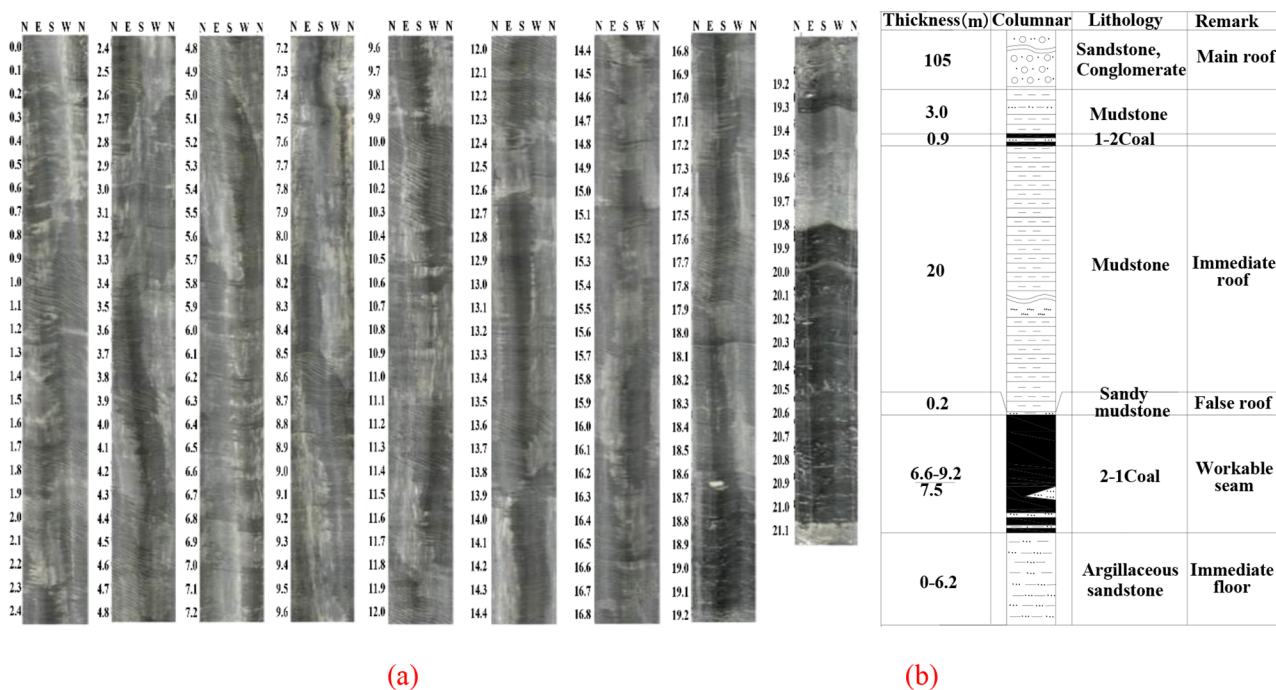
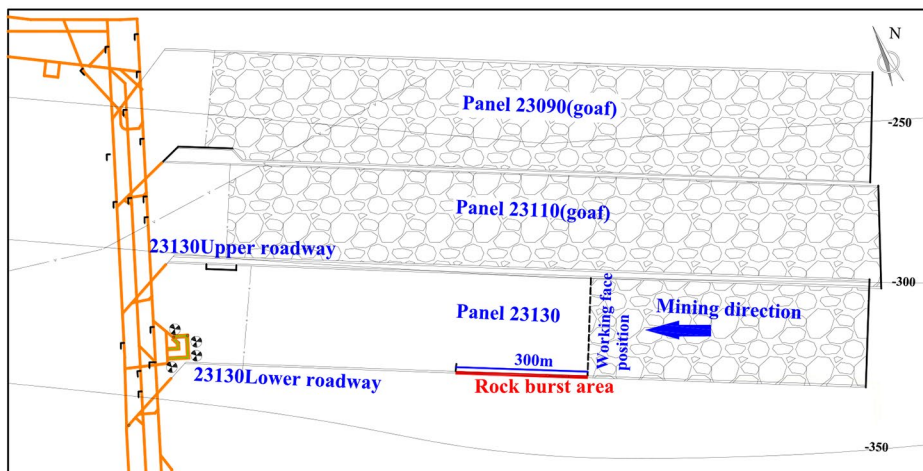
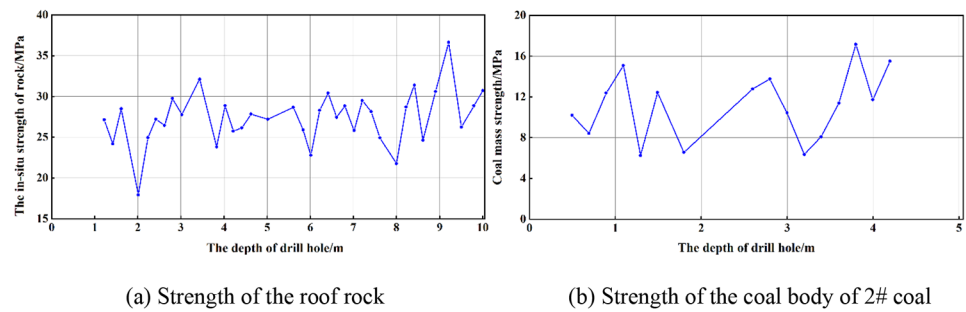


Fig. 2 The observation results of the belt transport roadways at 23130 working face

21 m is small coal. Combined with the comprehensive histogram of the roof and bottom slab of the coal seam at the 23130 working face (Fig. 2b), there is the immediate roof of coal seam with an average thickness of 25 m mudstone, the sandy false roof with a mudstone thickness of 0.2 m, the immediate floor of argillaceous sandstone with a thickness of 6.2 m and the hard floor with a thickness of 105 m of conglomerate.

The in-situ strength test results of the coal rock within 10 m of the roof of the belt transport roadways within the coal bank holes at 23130 working face are shown in Fig. 3. The strength range of the roof mudstone is 25–40 MPa, and

the average strength is 32.5 MPa. The fluctuation range of the strength value of the roof mudstone is relatively small, and the rock layer is more easily broken by dynamic load disturbance such as mining. The strength of the coal mass can reflect the degree of integrity itself. The strength of the deep coal body is generally greater than that of the shallow coal body for the coal bank. The deep part of the coal bank has better integrity but the shallow part is relatively broken. After calculation, the average strength of relatively intact No. 2 coal seam sample is 21.19 MPa, and the average strength of broken coal body of coal bank is about 11.47 MPa. It was found that the coal bank with better integrity is easy to

Fig. 3 Strength test curve of coal and rock at 23130 working face**Table 1** Ground stress test results in Yuejin Coal Mine

Name of mine	Point No.	Depth (m)	σ_H (MPa)	σ_h (MPa)	σ_v (MPa)	Maximum horizontal principal stress direction
Yuejin Coal Mine	1	1011	19.92	10.31	25.28	N82°W
	2	874	17.65	8.84	21.84	N87 °W
	3	872	15.27	8.24	21.80	N96°E
	4	873	17.37	9.11	21.83	N68 °W
Average value			17.55	9.12	22.68	-

produce energy accumulation during the mining process. In summary, the roof rock of the 23130 working face in Yuejin Coal Mine is easy to be broken, and there is a risk of accidents such as bottom drum, piece and puking.

Under the condition that the structural characteristics of the surrounding rocks and the in-situ strength of the coal rock body have been explored, the in-situ stress test results of Yuejin Coal Mine are shown in Table 1 (Jiao 2017). The Yuejin coal mine is in a gravity-type high stress zone dominated by vertical stress, that is, vertical principal stress > maximum horizontal principal stress > minimum horizontal principal stress ($\sigma_v > \sigma_H > \sigma_h$). As the main mining seam is located at deep area, the ground stress is high and the pressure is relatively obvious. The maximum horizontal principal stress is generally in the NW direction with an average of about 83°. In such a high ground stress environment, the top plate of 23130 working face is loose and easily broken mudstone. Moreover, the roof of the measurement point and the two banks have different degrees of fissures and delamination. Therefore, large deformations are easily generated in the stope drift active workings, and rockburst is prone to occur due to the influence of mining.

2.3 Overview of rockburst accidents at the 23130 working face of Yuejin Coal Mine

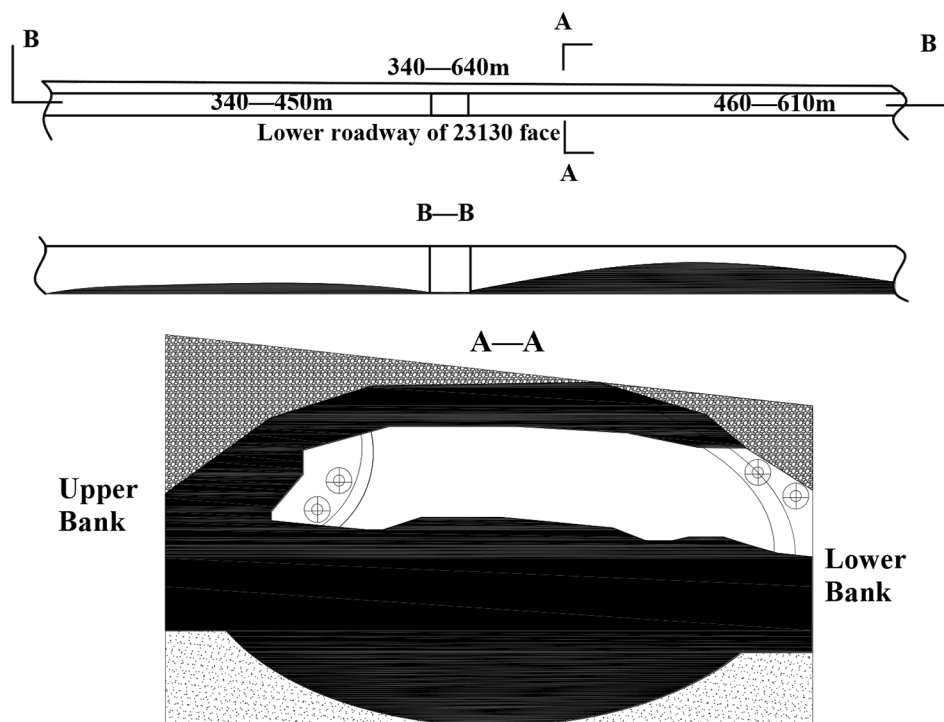
The 23 mining area of Yuejin Coal Mine is mainly for deep mining, and the coal rock body is in a high stress environment. When the strength limit of rock destruction is not reached, the coal rock mass deforms violently and simultaneously forms a high-energy carrier that accumulates a lot of elastic energy. The high-energy carrier can easily induce rockburst under the influence of mining activities or other geological activities. According to statistics, 21 times of

rockburst occurred during the workings back in the No. 23 mining panel, which brought huge economic losses to the coal mine. Among them, when the 23130 working face was mined to 360 m, the most intense rockburst occurred in the lower road (the belt transport roadway, as shown in Fig. 1) of the working face, which caused the most serious damage. The total length of the belt transport roadway of the 23130 working face is 1007 m, and the section shape is oval with a major axis of 6.2 m and a minor axis of 5 m. The roadway is arranged in 2–1 coal seam and excavated along the roof of the coal seam. The composite support of “Anchor Mesh Cable+elliptical shed” is adopted, which is mainly used to provide fresh air flow for the mining of the working face.

In the 340–640 m section of the lower roadways of 23130 working face, this rockburst led to different ranges of damage including the roof of the roadways caving, the upper coal wall flaking, and the floor bulging seriously and so on. Many mining equipment were also damaged, and the roadway of about 300 m long was affected by the rockburst. According to the ESG microseismic monitoring system, this rockburst occurred in the coal seam with an energy of 4.1×10^5 J and a magnitude of 1.1. A cross-sectional view of the destruction of the belt transport roadway in the 23130 working face along the roadway axis and the coal seam inclination is shown in Fig. 4.

From the B-B profile in Fig. 4, it is obvious that the deformation and failure of the roadway in the 23130 working face is mainly the floor bulging failure after the rockburst. The 460–610 m section of the roadway in front of the work face is severely deformed, which is manifested by the obvious reduction and deformation of the roadway section. In the section of the roadway, a large number of coal seams are thrown along the floor of the roadway, with the lowest net height of 1.4 m and the narrowest net width of 2.3 m,

Fig. 4 Damage profile of the 23130 lower roadway



while the net height of other roadways is above 1.7 m. In the 340–450 m section of the roadway, the bottom slab also deforms with the 0.1–0.6 m bulging floor. There is almost no deformation in the 450–460 m section of the roadway. From the on-site inspection, various equipment in the lower roadway are crumbled over, and the protective sponge mats are all crumbled off to the bottom plate. Some single pillars are collapsed and bent, and various pipelines in the roadway are damaged to varying degrees. In general, the farther away the working face is from the front, the smaller the amount of roadway destruction and deformation. From the B-B profile in Fig. 4, it can also be concluded that the damage of the roadway is mainly manifested as floor bulging damage. A large amount of coal is also thrown out on the roof and upper bank, and the direction of the coal body is thrown along the coal seam. The deformation of the lower shed beam is not obvious, and there is almost no damage in the range of the roof of the roadway.

The analysis of the site investigation accident report shows that the overhanging area of the main roof above the goaf of the 23130 and 23110 working faces in the No. 23 mining panel is square, and the working faces have entered the “double square” stage, which increases the pressure on the key layer of the main roof. The cracking and falling of the main roof are the main reasons for this rockburst. Before the rockburst, continuous multiple pressure relief blasts from 655 to 688 m in the 23130 lower roadway (the blasting area is less than 50 m from the rockburst area) provided dynamic disturbances for the occurrence of rockburst. However, it

is obviously not sufficient to qualitatively analyze the reasons for the rockburst occurring in the process of mining at 23130 working face only from the appearance characteristics and the temporal and spatial position and surrounding rocks structure characteristics of the working service face and the adjacent mining face of the burst stope drift active workings. In fact, the mechanism of rockburst is extremely complicated. As a special form of mineral pressure manifestation, due to the dynamic load of the trigger event, a large amount of elastic energy accumulated in the coal and rock mass under high stress conditions is suddenly and violently released into the excavation space in the form of vibration, sound and coal mass ejection. For the rockburst accident, what are the stress states and distribution characteristics of coal and rock masses? What are the energy accumulation characteristics of coal and rock volume before burst and the change law of energy released from different sections of roadway during burst? What is the change of stress state of roadway surrounding rock when the disturbance source (main roof collapse and pressure relief blasting) induces burst? Even before the critical burst failure of the surrounding rocks of the roadway, is there a rule to follow for the change of the plastic failure area? This series of issues still needs further study.

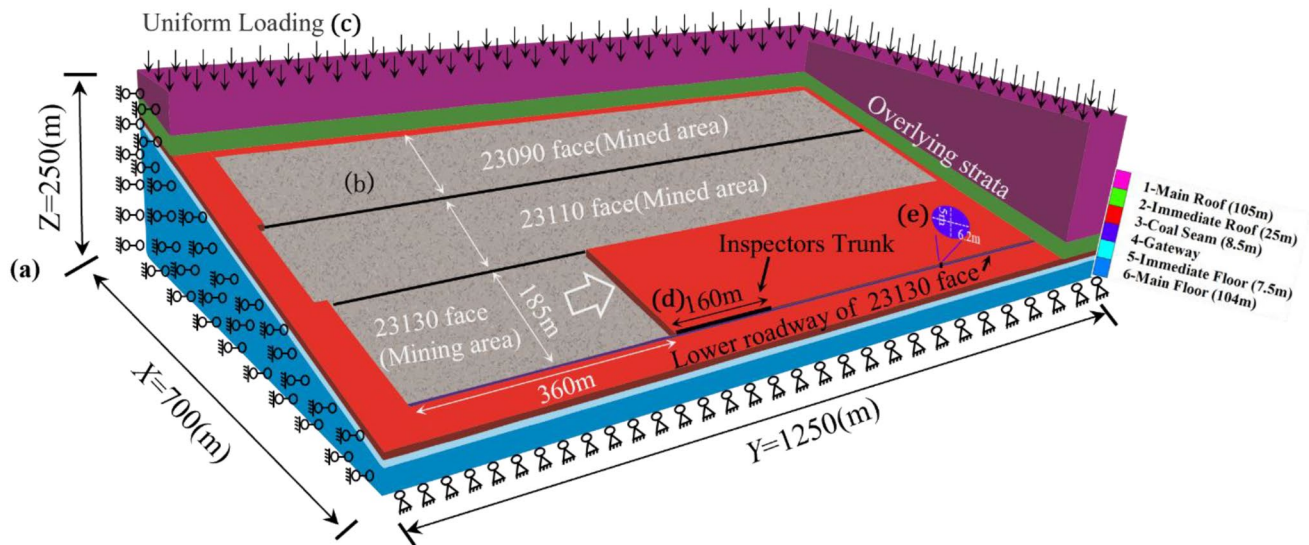


Fig. 5 Three-dimensional numerical analysis model and working surface layout

3 Numerical simulation of the rockburst in the lower roadway of 23130 working face

On the conditions that the deep in-situ stress environment of Yuejin Coal Mine, the excavation replacement layout, surrounding rocks structure characteristics and strength information in the working face and service roadway of the No. 23 mining area are explored. The numerical simulation of the preparation and occurrence process of rockburst in the lower roadway of 23130 working face is carried out in order to reveal the occurrence mechanism of rockburst in the mining roadway.

3.1 Numerical model

Combining with the geological data and the actual mining situation of the No. 23 mining area before the occurrence of rockburst in the lower roadway of 23130 working face, FLAC^{3D} 6.0 numerical simulation software is applied to construct a three-dimensional numerical model. The three-dimensional numerical model contains 3,623,520 grid elements and 3,699,109 nodes, and the size is 700 m × 1250 m × 250 m, as shown in Fig. 5. The simulated rock layers are arranged according to Fig. 2b, and the model rock layer structure is appropriately simplified. The average buried depth of the coal seam in the 23130 working face is 830 m, and the lower roadway is located in the coal seam and arranged along the coal roof. According to the actual situation, the roadway section is properly set and the working face inclination is set to 12°. In the numerical model, it is stipulated that the coal seam inclination direction is the X-axis direction, the advancing direction along the working face is the Y-axis direction, and the vertical direction is

the Z-axis direction. The overlying unsimulated rock layer is replaced by a uniformly distributed load, which is the weight of the overlying rock layer, that is, $\sigma_Z = \gamma H = 0.025 \times 700 = 17.5$ MPa (the average bulk density of the overlying rock layer is 25 kN/m³). The boundary conditions of the numerical model are set to a fixed horizontal displacement on the X-axis and Y-axis boundaries, and a fixed vertical displacement on the lower boundary of the Z-axis. The initial stress field of the model is applied according to the average value of the measured ground stress in Yuejin Coal Mine in Table 1, namely $\sigma_{XX} = 17.55$ MPa, $\sigma_{YY} = 9.12$ MPa, $\sigma_{ZZ} = 22.68$ MPa. The Mohr-Coulomb failure criterion is used for calculation, and in order to better simulate the surrounding rock stress environment of the actual 23130 working face during pushing and mining, three working faces 23090, 23110 and 23130 are arranged. According to the test results of mechanical properties of coal and rock in the lower roadway of 23130 working face (relevant data obtained from laboratory test after drilling and sampling on site) and mine geological data (Hao 2018; Jiao 2017), an appropriate reduction is made. The specific mechanical parameter settings of coal and rock mass are shown in Table 2.

3.2 Simulation scheme

In view of the occurrence of rockburst, the mining at the 23090 and 23110 working faces has already been completed. Combined with the actual production connection of the No. 23 mining areas, the numerical simulation mining scheme is divided into 4 steps. The first step is to perform the balance calculation of the initial geostress environment. The second step is to stop the 23090 working face to perform the balance calculation. The third step is to stop the

Table 2 Numerical simulation of rock mechanics parameters

Lithologic map	Thickness (m)	Density (kg/m ³)	Bulk modulus (GPa)	Shear modulus (GPa)	Cohesion (MPa)	Internal friction angle (°)	Unidirectional tensile strength (MPa)	Dilatancy angle (°)
Main roof sandy conglomerate	105.0	2680	9.56	8.35	12.3	36.4	3.69	-
Immediate roof mudstone	25.0	2430	4.36	3.41	4.2	30.7	1.86	-
2–1 Coal	8.5	1350	1.28	0.81	3.4	27.0	1.13	-
Immediate floor sandy mudstone	7.5	2510	7.17	5.14	6.2	31.8	2.45	-
Main roof sandstone	104.0	2720	9.86	8.64	15.3	35.2	4.52	-
Filling body	8.5	1800	6.86	5.53	-	20.0	-	7

23110 working face to perform the balance calculation. The fourth step is to perform balance calculation when the 23130 working face is mined to 360 m. In all working faces of the No. 23 mining area, all caving methods are used to deal with the goaf during mining. Double-yield is suitable for numerical simulation of rock and soil materials that will produce irreversible compression deformation and shear yield, so it can be used for simulation calculation of filling goaf and caving zone (Salamon 1990; Zhou and Zhu 2010). Therefore, in this work, the Double-yield constitutive model is selected to fill the goaf formed by excavation. The goaf formed by the model is filled in every step of the excavation, and the filling mechanics parameters are shown in Table 2.

It can be seen from Fig. 5d that the monitoring line is extended along the advancing direction at a distance of 360 m from the open-off cut in the lower roadway of the 23110 working face, and the length of which is 160 m. Then, a measuring point is set every 5 m along the monitoring line to monitor the mining stress field and surrounding rock plastic failure distribution characteristics when the 23110 working face is mined to 360 m.

3.3 Results

3.3.1 Distribution characteristics of the mining stress field when the working face advances to 360 m

The existing research results show that a vertical bearing pressure zone will be formed around the mining space, and the peak mining stress in this area can reach 2 to 5 times the original rock stress. Meanwhile, the decompression zone extending outward from the supporting pressure zone is also subject to the superimposed influence caused by the excavation activities of the adjacent goaf or working face. The concentration of mining stress caused by this superimposed influence is one of the main reasons for coal and rock dynamic disasters such as rockburst. According to statistics, more than 75% of the burst damage occurs in the roadway, especially within the range of 0–80 m from the working face (Hao 2018). However, the stress in the actual mining process is unpredictable. Sometimes, the maximum principal stress

in the mining roadway area is not in the vertical direction, but has a certain angle with the vertical direction. Because of that, when the 23130 working face is mined to 360 m, in order to analyze the actual distribution characteristics of the mining stress field of the coal and rock mass in the area around the lower roadway, slices are made along the coal seam inclination of the numerical model, and the distribution characteristic cloud map of the regional principal stress field is drawn (Fig. 6a). Then, some key data are extracted from Fig. 5d to draw Fig. 6b. They include the maximum principal stress P_1 is in the area within 160 m away from the emergency exit when the axial direction of the lower roadway of 23130 working face is pushed to 360 m, the minimum principal stress P_3 , angle between the P_1 and the Z-axis, and the calculated ratio η of P_1 to P_3 .

As shown in Fig. 6b, the P_1 , P_3 and the included angle show a sharp increase first, then gradually decrease and tend to be stable with the increase of the distance L/m to the working surface. And the severity of the change and the position of the peak appear different. P_1 reaches its maximum value at a distance of 10 m from the stopping position of the working face, which is 47 MPa. P_3 is 13.77 MPa at a distance of 10 m from the working surface, and it is 1/3.41 of P_1 . In addition, P_3 reaches the maximum at 15 m from the working surface, which is 14.99 MPa. As the distance to the working face increases, P_3 decreases slowly, and the magnitude of the decrease is less than P_1 . During the mining process at the working face, the principal stress direction is also deflected. The speed at which the angle between P_1 and the Z axis increases is greater than the speed at which it decreases far away from the working face. The speed is 2.8° at a distance of 10 m from the working face, and reaches its maximum value at a distance of 15 m, which is 2.0°.

Combined with the distribution characteristic map of the principal stress field from the 23130 working face to 360 m (Fig. 6a), it can be found that the “L-shaped” distribution of stress concentration areas is formed within 100 m of the 23130 work face. Influenced by the pressure relief in the goaf of the 23110 working face, the “triangular area” where the principal stresses are most concentrated is formed at the corner connecting the goaf of the 23130 working face with

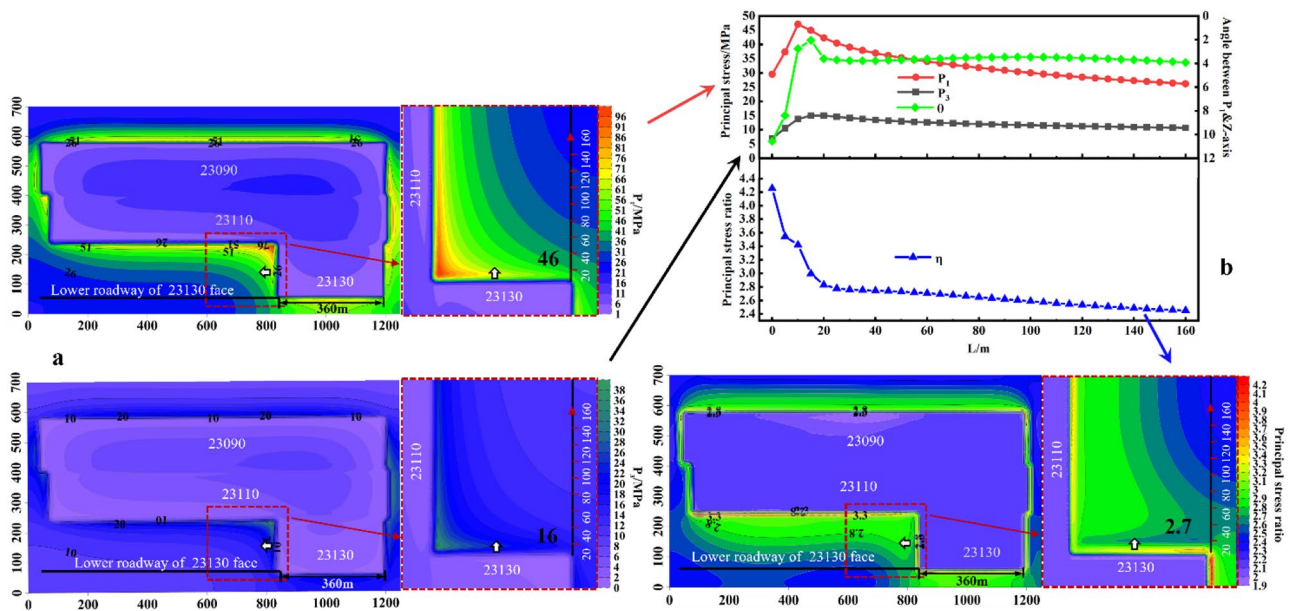


Fig. 6 The principal stress field around lower roadway in 23130 working face and axial roadway principal stress distribution curve

the goaf of the 23110 working face. Besides, the principal stress ratio of the principal stress field in the area within 100 m of the working front of 23130 working face is η , and $\eta = 2.59\text{--}4.26$. Based on the roadway butterfly damage theory and the Leau-Fatou petal inverse theorem in the non-linear dynamic system structure stability theory, the burst failure analysis of the entire surrounding rock system is carried out. The surrounding rock mass with the roadway as the center continues to change as the regional ground stress changes. When the maximum and minimum principal stress ratio η is close to or greater than or equal to 3, the surrounding rock mass will form an extremely unstable butterfly-shaped plastic failure zone, which is the 4-leaf petal pattern described by the Leau-Fatou petal inverse theorem. Moreover, this plastic failure form is highly sensitive to the surrounding stress and the behavior of the rock mass. Once the butterfly-shaped plastic damage is formed, the entire surrounding rock system is prone to instability mutation from the stable state to the burst damage (Ma et al. 2019a, b). Since the principal stress ratio $\eta = 2.59\text{--}4.26$ within 100 m in front of the roadway at the 23130 working face, it satisfies the stress condition for the formation of butterfly-shaped plastic damage zone in the surrounding rock of the roadway. This may be the “pre-state” stress environment before the rockburst occurred.

3.3.2 Distribution characteristics of the plastic failure of roadway surrounding rocks when the working face advances to 360 m

Based on the above analysis, we obtained the regional stress field and its distribution, and it is crucial to master the morphological characteristics of the plastic failure zone of the surrounding rock. According to the actual geological conditions of the roadway at the 23130 working face, cross-sectional slices are made along the axial monitoring line for the lower roadway of the 23130 working face, and the slices numerical analysis model is constructed. According to the Saint-Venant principle, the surrounding rocks are affected by excavation disturbance and gradually weakens as the distance between them and the roadway increases. Therefore, in order to avoid boundary effects affecting the accuracy of model calculations, the numerical model size of the entire roadway and surrounding rock is set to $200\text{ m} \times 200\text{ m} \times 1\text{ m}$. The horizontal and vertical boundary displacement of the model is fixed, and the normal displacement in the front and rear directions is fixed. Then, the model boundary stress is applied according to the magnitude and direction of P_1 and P_3 in Fig. 6b. The surrounding rocks part still adopts an ideal elastoplastic model that follows the Moore-Coulomb yield criterion, and the roadway excavation part uses zero element simulation. There are detailed physical and mechanical parameters of rock formations in Table 2.

When the 23130 working face advances to 360 m, the principal stress ratio η , the principal stress direction θ and the morphological characteristics of the surrounding rock plastic failure zone within 100 m in front of the 23130 roadway

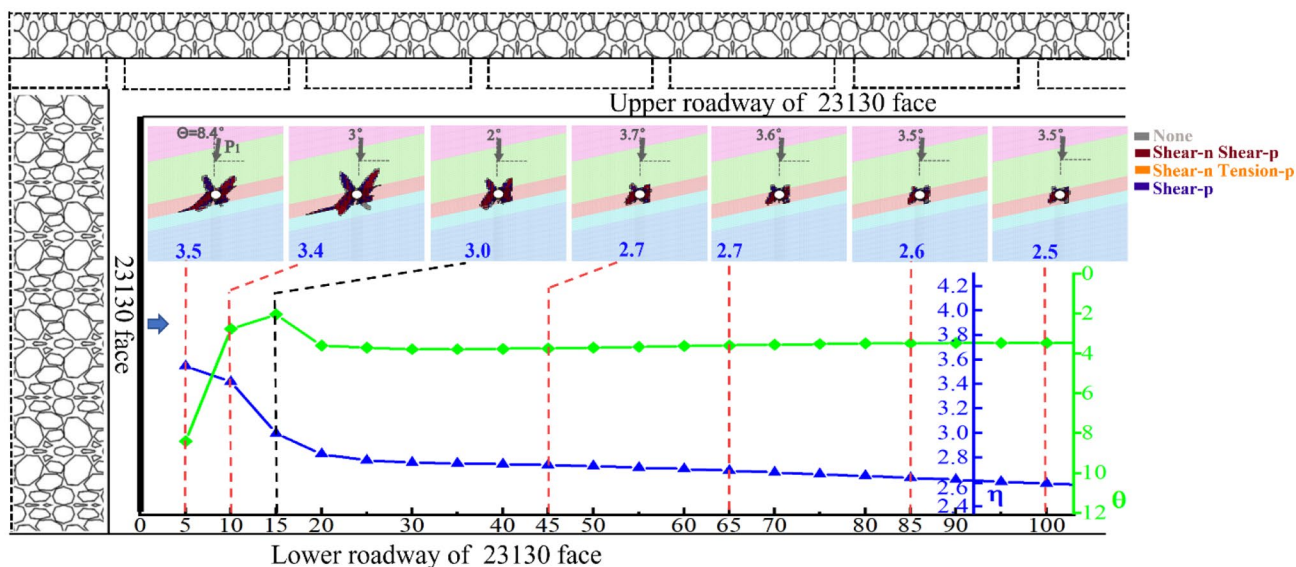


Fig. 7 Change of morphological characteristics of plastic zone with working face distance L

are shown in Fig. 7. It can be seen from the Fig. 7 that, under the stress environment with $\eta = 2.59\text{--}4.26$, butterfly-shaped plastic failure is formed around the roadway. And the failure mode is the “pre-state” failure range before the occurrence of rockburst. With the difference of the distance to the working face, the plastic failure characteristics of the surrounding rock show obvious differences. On the one hand, when the working face is far away (the distance is 65 m, 85 and 100 m), η is generally less than 2.8, and the deflection of θ is concentrated at about 3.5° . In this range, the plastic zone range of the surrounding rocks of the roadway changes significantly with the deflection of θ , and the damage is mainly concentrated at the shoulder corners of the roof and floor of the roadway. In addition, the plastic zone of the floor is obviously larger than that of the roof, and the characteristic that the plastic zone is butterfly-shaped distribution is not obvious. On the other hand, as the distance to the working face decreases, the plastic zone at the shoulder corner of the roof and floor of the roadway gradually expands to the deep part, and the expansion speed of the plastic zone on the roof is significantly faster than that of the floor. At a distance of 15 m from the working face, η is close to 3.0, and θ is deviated by about 2° . The plastic zone has formed obvious butterfly failure, and the plastic failure range at the shoulder corner of the roof and floor of the roadway is close. In addition, due to the influence of the main stress direction θ , the butterfly blade deflection occurs, and the left shoulder corner of the floor has a larger range. It can be concluded that the morphological characteristics of the plastic zone are significantly affected by the magnitude and direction of the principal stress in the surrounding area, and the morphological characteristics of the plastic zone and the maximum size

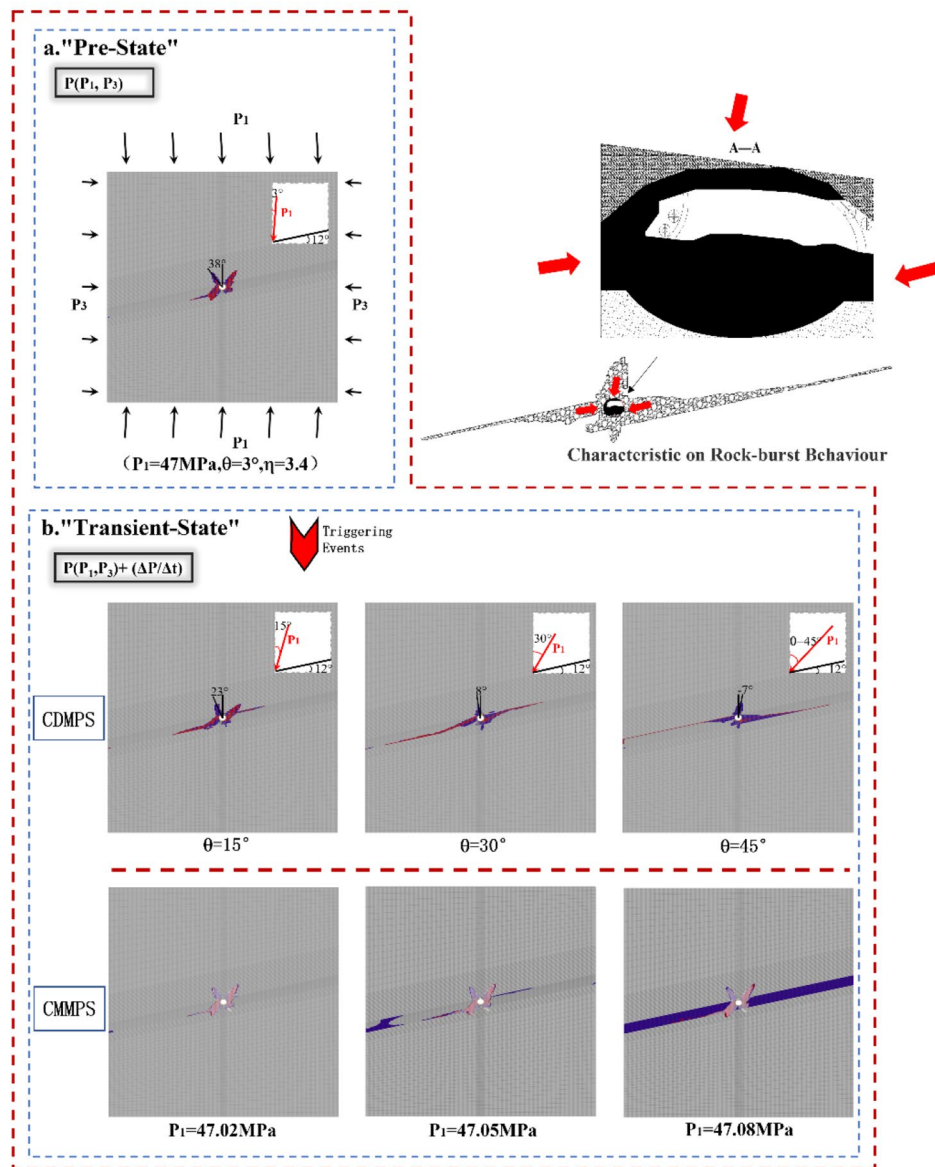
position of the plastic zone will change with the change of the principal stress direction.

Through the analysis of the distribution characteristics of the mining stress field and the shape change of the plastic failure zone of the surrounding rocks of the roadway when the 23130 working face advances to 360 m, it can be known that the surrounding rock mass is subjected to a high deviatoric stress field within a range of 100 m before the occurrence of rockburst in the lower roadway of the 23130 working face, and the principal stress ratio $\eta = 2.59\text{--}4.26$. The plastic failure zone of coal and rock mass is a butterfly-shaped failure form. Besides, the closer to the working surface, the more significant the butterfly damage and the larger the range, and the greater the risk of rockburst. Overall, the relatively stable “pre-state” formed by the high-stress environment and the butterfly-shaped failure of the coal and rock masses is the precursor of the burst and catastrophe of the coal and rock masses around the roadways of the 23130 working face.

3.3.3 “Transient” burst catastrophic characteristics under dynamic disturbance

As mentioned in the above accident overview, the area where the rockburst appears most severely at the 23130 working face is the Sects. 460–610 m in the lower roadway. Moreover, the numerical simulation results show that this area is a “pre-state” composed of the high principal stress environment and the butterfly-shaped plastic failure range of the surrounding rocks. The dynamic disturbance ΔP produced by the rupture of the main roof or the pressure relief blasting is the triggering event that leads to the

Fig. 8 “Transient” catastrophe process when rockburst occurs. Note: CDMPS represents “Change the deflection direction of the maximum principal stress”; CMMPS represents “Change the magnitude of the maximum principal stress”



instantaneous instability of the entire “pre-state” system. Namely, the “pre-state” is affected by the dynamic load disturbance, and the surrounding rock system of the roadway area changes from the relatively stable “pre-state” before the rockburst to the “transient” instability when the rockburst occurs. “Transient” also includes the characteristics of transient stress field and the range of transient rock mass plastic failure. “Pre-state” refers to the stress field formed by the superposition of the triggering event and the previous state stress field, namely $P(P_1, P_3) + \Delta P$. “Transient” refers to the damage range generated by the surrounding rock of the roadway at the time of rockburst, which is the mechanical response to the transient stress field (Fig. 8).

Combining the Fig. 7, and taking the “pre-state” butterfly plastic failure zone 10 m away from the working face as an

example, the butterfly leaves are located at the four shoulder corners of the roadway. If the disturbance induces burst damage in this state, it will inevitably cause the coal and rock masses to be suddenly thrown into the roadway in the four shoulder corner areas, and the entire roadway section will be severely closed and deformed. However, in fact, the most serious damage feature of the roadway burst is that the roadway section is significantly reduced and deformed, and the coal seam is thrown out in large quantities along the floor (as shown in *A-A* section of Fig. 4). Therefore, this conclusion can be drawn that when the dynamic disturbance source (the main roof collapsing and pressure relief blasting) induces a burst, the direction of the transient stress field must change. The magnitude and direction of the dynamic disturbance directly affect the change of “transient” plastic

failure, that is, the failure form of rockburst. Therefore, a comprehensive study on the change characteristics of the transient plastic failure zone when the magnitude and direction of the principal stress change will help to obtain the real stress field characteristics and transient failure mode when the dynamic disturbance source induces burst. From the Fig. 8a, it can be found that since the maximum principal stress of the surrounding rock of the roadway appears at a position 10 m away from the working face, and the principal stress ratio $\eta = 3.41$, a large-scale butterfly plastic failure has been generated in the “pre-state”. As shown in Fig. 8b, due to the sensitive dependence of butterfly failure under this stress state, the change characteristics of the “transient” plastic failure zone during burst are simulated under the condition of only changing the deflection direction of the principal stress. It can be concluded that the butterfly blade in the butterfly-shaped plastic failure zone not only deflects significantly with the direction of the maximum principal stress, but also expands malignantly. The deflection angle of the butterfly-shaped plastic failure butterfly blade and the principal stress direction is basically the same. Especially when the direction of the maximum principal stress is deflected by about 45° , the burst appearance characteristics of the malignant expansion of the butterfly-shaped plastic zone are closer to the failure characteristics of the actual roadway section. In addition, by controlling the direction of the maximum principal stress to remain unchanged and only changing the magnitude of the maximum principal stress (setting the principal stress perturbation equals to 0.2, 0.5, 0.8 MPa/s), it can be found that the dynamic disturbance of 0.2 MPa/s formed a transient stress field, which caused the expansion of butterfly damage. The dynamic disturbance of 0.2 MPa/s formed a transient stress field, which caused the expansion of butterfly damage. The dynamic disturbance of 0.5 MPa/s can already extend the butterfly failure and cause large-scale rupture in the weak coal seam where the roadway is located. When the dynamic disturbance is 0.8 MPa/s, plastic failure occurs in the whole coal seam. Based on the above analysis, the dynamic disturbance caused by the collapse of the main roof or the pressure relief blasting is extremely complicated. This dynamic disturbance not only changes the size of the stress field of the surrounding rock of the roadway, but also changes the direction of the stress field, which makes the plastic failure zone of the surrounding rock of the roadway deflection and malignant expansion when the rockburst occurs. In order to analyze the plastic failure characteristics of the surrounding rock of the roadway within 100 m from the working front, the study was carried out under the condition of $\Delta P = 0.2$ MPa/s and the expansion of the plastic zone under the transient stress field formed by the maximum stress direction deflection 45° .

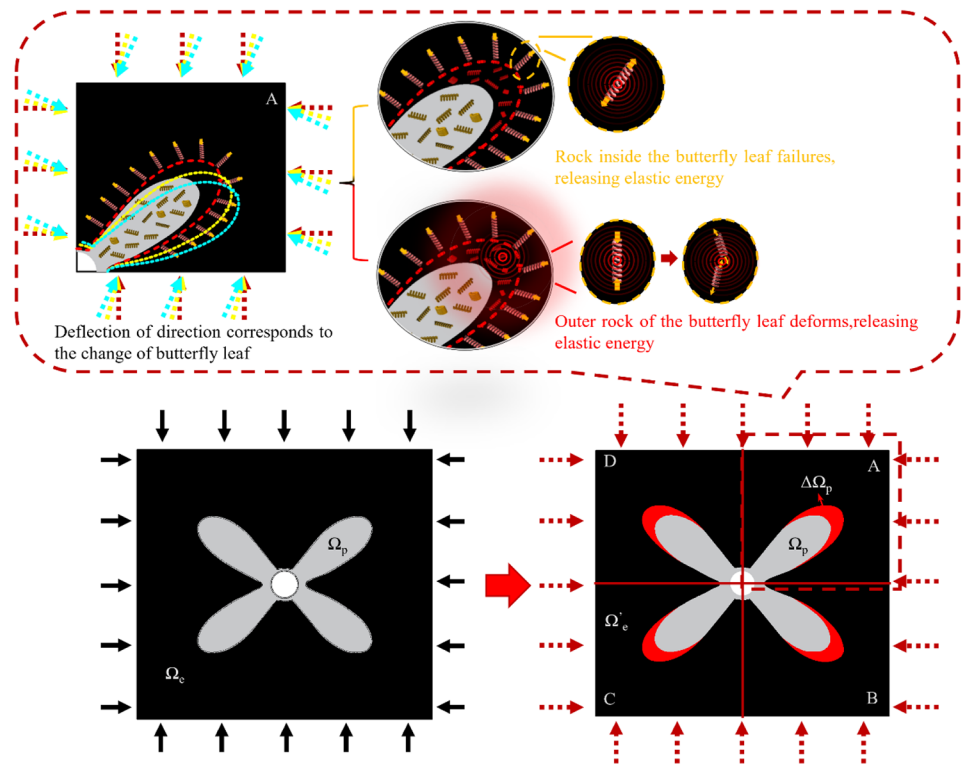
In summary, the occurrence process of rockburst is extremely complex and nonlinear. The forward simulation method is used to simulate the damage characteristics and stress field distribution of the surrounding rock of the roadway before the rockburst occurs. This nonlinear dynamic process is manifested as: under the action of a triggering event, the “pre-state” butterfly plastic failure of the surrounding rock in the roadway transforms into a “transient” butterfly blade deflection and bursting expansion. According to the law of thermodynamics, the essential feature of material destruction is a state instability phenomenon in the process of energy conversion and transfer. In the dynamic process of real rockburst, the accumulation and release of elastic energy often occur. Therefore, in order to clarify the occurrence mechanism of rockburst in the stope drift active workings, it is necessary to study the distribution characteristics and accumulation and release laws of elastic energy before and after the occurrence of rockburst.

3.3.4 The law of energy accumulation and release before and after the burst of the lower roadway in 23130 working face

The elastic energy contained in the rock mass in the “pre-state” failure zone is called “internal energy”. Its value depends on the mechanical properties of the rock mass (elastic modulus E , Poisson’s ratio μ) and principal stress distribution in the failure zone. The regional rock mass within the “pre-state” butterfly-shaped failure boundary can either be in a broken state with load-bearing effect, or it can be separated into several large pieces of broken rock mass. Part of the elastic energy is still stored outside the butterfly failure boundary. This part of the elastic energy is called “system energy”, which can be calculated by the mechanical properties (elastic modulus E , Poisson’s ratio μ) of each rock formation and its stress distribution. As a result of the triggering event, the sudden release of “internal energy” and part of “system energy” is stimulated, which causes the occurrence of “transient state” of rockburst. This process causes the supporting effect of the rock mass on the butterfly-shaped failure boundary to fail completely or partially in an instant. The nearby rock mass is compressed to the inner space of the butterfly failure, which causes the expansion of the butterfly failure or the chain failure of a certain range of rock mass.

As shown in Fig. 9, the butterfly plastic failure zone (gray and expanded red zone) under the action of transient stress field is symmetrically divided into four areas A, B, C, and D with the center of the roadway as the origin. Taking the area B as an example, the dynamic physical process of the expansion of the rupture zone of a single butterfly leaf is analyzed with the release of energy (the amount of released energy is

Fig. 9 The dynamic energy release process of rockburst caused by butterfly failure and expansion



not specifically discussed here). Due to the triggering event, the stress state around the rupture zone has changed, causing the gray rupture zone to expand and form a new failure zone (red area). Taking the red dotted line as the boundary, the released energy is mainly composed of the elastic energy released by the internal rock failure and the external rock deformation in the fracture zone. The energy accumulated in the rock inside the dotted line boundary in the red box is damaged because it cannot bear the current stress state. This process of energy release can be seen as countless springs breaking when they exceed their load-bearing capacity. At the same time, there is still a large amount of elastic energy accumulated at the boundary of the newly formed damaged area. As this elastic energy continues to squeeze the newly formed failure zone, the rock outside the boundary of the zone undergoes elastic deformation and releases a large amount of elastic energy. This part of the energy release can be regarded as the “elastic rebound” of the external spring. Consequently, the abrupt expansion of butterfly damage will cause rock damage inside the damage zone and release a certain amount of elastic energy. Meanwhile, the rock outside the butterfly-leaf boundary is elastically deformed and releases another part of the elastic energy (Fig. 9). The elastic energy of the inner and outer parts of the butterfly-shaped plastic failure zone on the surrounding rock of the roadway is released simultaneously, which will trigger the rockburst originated from the formation of the fracture expansion zone. In other words, the energy of rockburst comes from

the elastic energy around the butterfly-shaped plastic failure zone of the surrounding rock of the roadway. Besides, the released elastic energy is the sum of the elastic energy released by the transient expansion of the butterfly leaf and the elastic deformation energy of the rock around the failure zone.

As shown in Fig. 9, the “internal energy” and “system energy” described by the dynamic release of elastic energy during the nonlinear dynamic process of rockburst are expressed by formulas. And the sum of the “system energy” and “internal energy” of the “pre-state” is represented by W_1 . The relationship can be obtained as follows,

$$W_1 = \iiint_{\Omega_{\{P_1, P_3\}}} f(x, y, z) dV - \left[\iiint_{\Omega_e} f(x, y, z) dV_e + \iiint_{\Omega_p} f(x, y, z) dV_p \right] \quad (1)$$

where,

$$f(x, y, z) = f(\sigma_{1,i}, \sigma_{2,i}, \sigma_{3,i}) = \frac{1}{2E_i} [\sigma_{1,i}^2 + \sigma_{2,i}^2 + \sigma_{3,i}^2 - 2\mu_i(\sigma_{1,i}\sigma_{2,i} + \sigma_{2,i}\sigma_{3,i} + \sigma_{3,i}\sigma_{1,i})] \quad (2)$$

where E_i and μ_i are the Young’s modulus and Poisson’s ratio of any mineral particle i . $f(\sigma_{1,i}, \sigma_{2,i}, \sigma_{3,i}) \cdot \Delta V_i$ is the elastic energy of the mineral particle i . The elastic energy of the entire region Ω is the triple integral of the function $f(x, y, z)$ on the bounded closed region Ω . $\Omega_{\{P_1, P_3\}}$ is the elastic property of the rock mass in the study area under the pure elastic state with the principal stress of $\{P_1, P_3\}$.

When the trigger stress is applied, the rock mass forms a new fracture area $\Delta\Omega_p$, which must release part of the elastic energy W_m in the form of elastic waves. In theoretical calculations, in order to accurately represent the process of triggering the event to generate a new fracture zone and release the elastic energy of the rock mass under the same stress state, it is necessary to calculate all the elastic energy released by the rock mass at $\{P_1 + \Delta P, P_3\}$ (the regional maximum principal stress is $P_1 + \Delta P$, and the minimum principal stress is P_3) again, namely the “system energy” + “internal energy” of “transient”, expressed by W_2 as follows,

$$W_2 = \iiint_{\Omega_{(P_1+\Delta P, P_3)}} f(x, y, z) dV - \left[\iiint_{\Omega'_e} f(x, y, z) dV'_e + \iiint_{\Omega_p+\Delta\Omega_p} f(x, y, z) d(V_p + \Delta V_p) \right] \quad (3)$$

obviously, as shown in Eq. (3), the total elastic energy W_2 released when the force state of the rock mass is $\{P_1 + \Delta P, P_3\}$ is greater than the elastic energy W_1 released when the force state of the rock mass is $\{P_1, P_3\}$. By making the difference between W_2 and W_1 , due to the triggering stress, all the elastic energy released by the newly generated fracture zone $\Delta\Omega_p$ in the rock mass can be obtained. This part of elastic energy is transformed and transferred into various forms of energy, such as the dissipated energy of mechanical behavior like rock deformation and micro-defect penetration, rock kinetic energy and frictional heat energy and so on. Among them, only a part is converted into elastic wave radiation energy W_m , that is, the energy released when the rockburst “transient” occurs. Since the relationship between different forms of energy is still unclear, for simplicity, an energy conversion factor β ($0 < \beta < 1$) is assumed, as follows,

$$W_m = \beta \times (W_2 - W_1) \quad (4)$$

The elastic energy of the in-situ rock mass is calculated twice under the force state of $\{P_1, P_3\}$ (the current stress state “pure elasticity” and “elasticity + rupture”), and the elastic energy is calculated twice under the force state of $\{P_1 + \Delta P, P_3\}$ (the current stress state “pure elasticity” and “elasticity + rupture”). The difference between the two calculated elastic energies is multiplied by the energy conversion factor β .

Applying Eq. (4), the characteristics of elastic energy accumulation and release are calculated ($\beta = 0.5$), as shown in Fig. 10. It can be seen that the surrounding rock system of the roadway before and after the occurrence of rockburst contains a lot of elastic energy. The elastic energy of the entire system is distributed in layers according to lithological characteristics, and the elastic energy contained in the coal seam is the highest, especially the elastic energy concentrated in the rock mass around the roadway (Fig. 10a). As shown in Fig. 10a, the critically unstable butterfly

damage has accumulated a large amount of elastic energy inside itself, resulting in a butterfly energy concentration zone. When the burst occurs, the elastic energy accumulated within the butterfly damage and the surrounding rock system is sufficient to provide the dissipated energy required for the sudden expansion of the butterfly leaf, without the need for additional energy from the outside. The butterfly-shaped plastic failure system of the surrounding rock of the entire roadway has the energy self-sustaining characteristics of the catastrophic failure of the rock mass, and the sudden release of elastic energy caused by it can reach 107 J, which is equivalent to the local failure strength of a magnitude 1.9 earthquake. In other words, at 10 m before the 23130 working face, when the maximum principal stress P_1 reaches the maximum at 10 m before the 23130 working face and the previous principal stress ratio is 3.41, a trigger disturbance of 0.2 MPa per unit time and accompanied by the deflection of the transient maximum principal stress direction can produce an earthquake of magnitude 1.9, which is catastrophic to the destruction of the roadway space.

Under the same triggering disturbance and different working face distances, the elastic energy released and the relative change Δ_{max} of the maximum value of the plastic failure radius (unit: a, the long axis radius of the roadway is 3.1 m) by expansion of surrounding rock, as shown in Fig. 11. It can be seen from the calculation that the relative variation between the released elastic energy W_m and relative variation of maximum plastic failure radius ΔR_{max} is the same, that is, with the increase of working face distance, it tends to be stable and gradually decreases after sharp rise and fall. The area close to the working face (within 15 m in front of the working face, the principal stress ratio $\eta = 3.0$) has great destructiveness and high energy level. Especially in the section with significant butterfly plastic failure of surrounding rock within 15 m away from the working face, the damage characteristics caused by malignant expansion of butterfly leaves are more obvious. When rockburst occurs, the plastic failure range of surrounding rock of mining roadway tends to decrease steadily with the increase of working face distance.

4 Occurrence mechanism of rockburst in the mining roadway

The physical analysis model of rockburst mechanism in the mining roadway is presented in Fig. 12. In this work, the whole physical process of rockburst occurring in the mining roadway is discussed from the perspective of stress, roadway surrounding rock failure and energy accumulation and release. Then a physical analysis model was constructed to quantitatively describe the occurrence process of rockburst

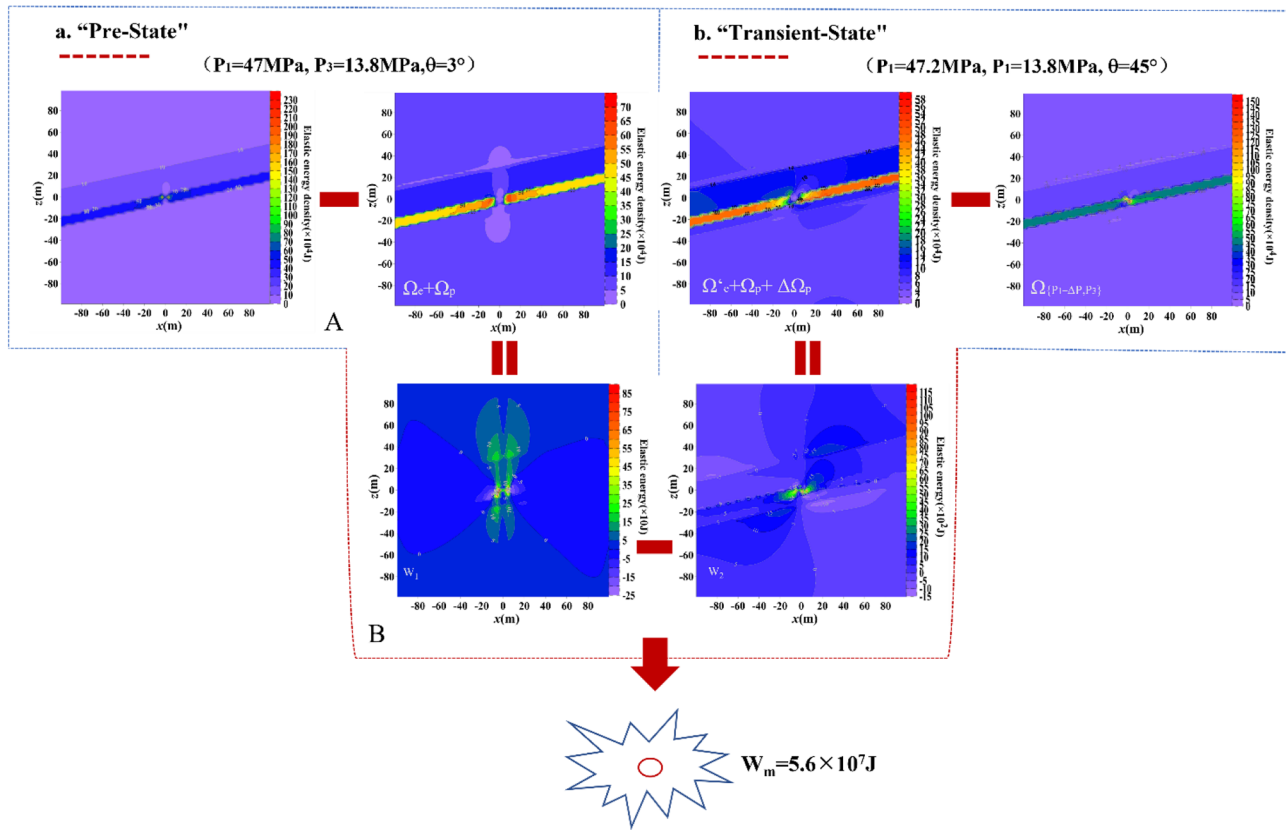


Fig. 10 Distribution characteristics and transformation relationship of elastic energy density of surrounding rock accumulation in the “pre-state” and “transient state” of burst

in the mining roadway. A new concept of “pre-state”, “transient state”, “trigger disturbance”, “internal energy” and “system energy” in the occurrence of rockburst in mining roadway is proposed. The physical connotations are as follows. In the process of deep coal mining, due to the complex and changeable high in-situ stress environment and sequential mining near the mined-out area, a high stress concentration area ($\eta = P_1/P_3 > 3$) is formed around the mining roadway. Under such a stress environment, the surrounding rock of the roadway will produce an extremely unstable butterfly-shaped failure zone (or incomplete butterfly), which will cause the accumulation of surrounding energy to form a combined energy field of “internal energy” and “system energy”. And this combined energy field together constitutes the “pre-state” of rockburst. Once it is subjected to the momentary action of triggering events such as the initial pressure and periodic pressure of the working face, the moving supporting pressure in front of the working face, the disturbance of the activation of the geological structure, and the excavation activities and so on, the butterfly-shaped damage zone will occur instantaneous and “pulsing” expansion or cause chain instability of nearby rock masses. Meanwhile, a large amount of elastic energy stored in the

butterfly-shaped failure zone and in the surrounding rock system is released in the form of vibration, sound, coal rock throwing, the bottom bulging, piece, the roof piking, and the roadway closure, which results in a dynamic phenomenon of explosive destruction. The appearance of the butterfly-shaped failure zone indicates that the surrounding rock system of the entire roadway is in a critical state of instability. Namely, the rockburst occurs “instantly”, and it is the “transient” instability of the “pre-state” butterfly failure under the sudden action of the triggering event, and the step response releases the “internal energy” and part of the “system energy”. In summary, the mechanism of the occurrence of rockburst in the mining roadway can be obtained as follows. During the mining process of the working face, if the damage zone of the surrounding rock of the mining roadway is butterfly-shaped, under the effects of instantaneous disturbances such as local excavation disturbance and geological structure activation, the butterfly-shaped damage zone has undergone large-scale transitional expansion. Along with this process, the butterfly-shaped failure zone releases elastic energy, which manifests as an explosive nonlinear burst dynamic phenomenon in the form of vibration, sound, coal and rock mass throwing, and roadway closure.

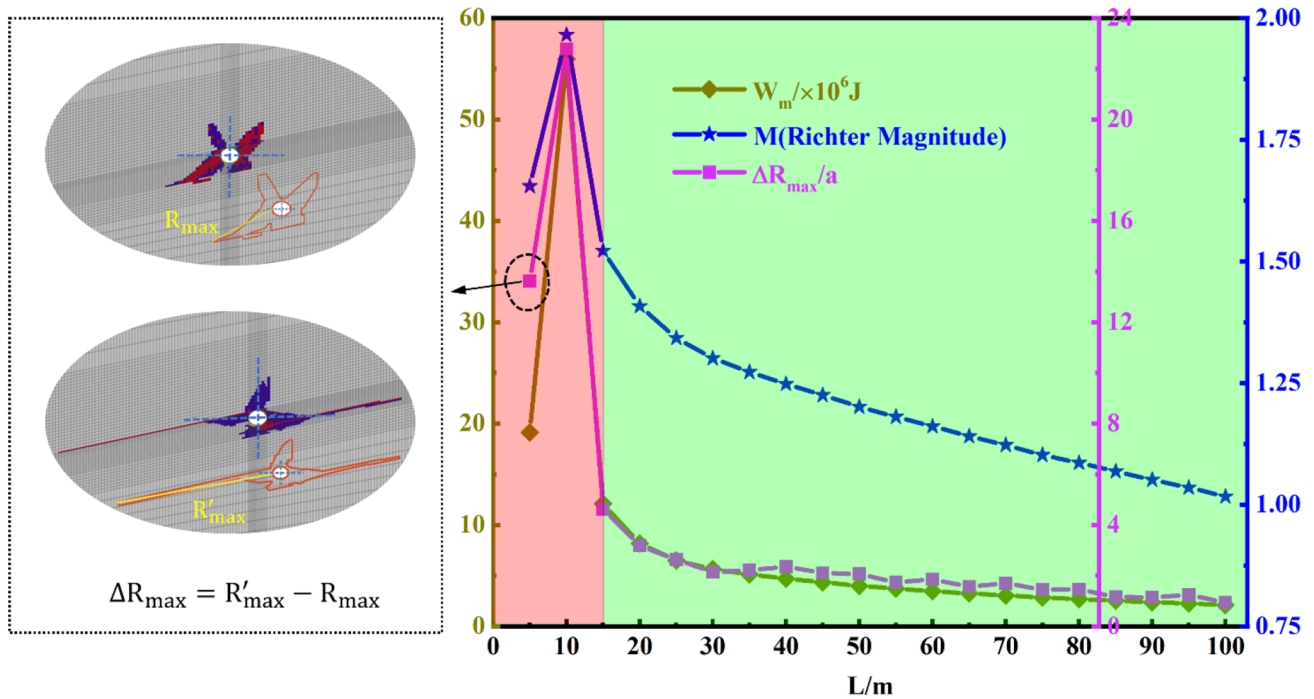


Fig. 11 Variation curve of Relative change maximum value of the plastic failure radius ΔR_{max} , Elastic energy released and corresponding Richter magnitude with working face distance L

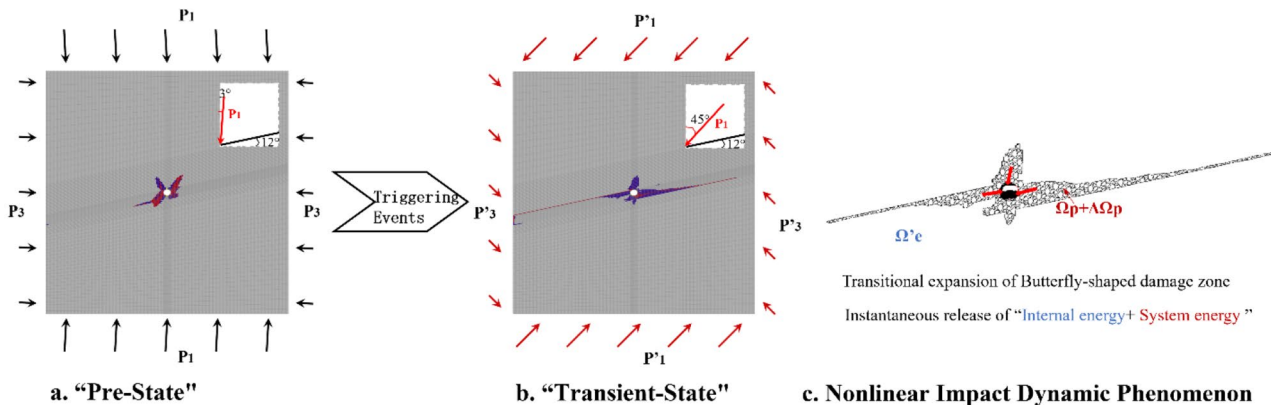


Fig. 12 Physical analysis model of rockburst mechanism in the mining roadway

5 Conclusions

(1) The change in the direction of the principal stress has a significant influence on the characteristics of the burst. With the increase of the working face distance, the dynamic expansion of the failure boundary radius show nonlinear change law that tends to be stable and gradually decreases after sharp fluctuation.

(2) The essential reason for the occurrence of rockburst in the mining roadway is the extremely unstable butterfly-shaped plastic failure of the surrounding rock in the

environment where the maximum principal stress and the minimum principal stress ratio of the area are close to or greater than 3. Under static or dynamic disturbances, when the butterfly-shaped failure boundary rock mass exceeds its own strength limit, the butterfly-shaped failure will destabilize and expand. Meanwhile, the release of elastic energy will cause the coal rock to be thrown into the roadway space and the roadway is closed.

(3) A calculation method for accumulating and releasing energy of rockburst is proposed. The release energy characteristics of burst failure obtained by simulation show a

nonlinear exponential decreasing trend with the increase of working face distance.

(4) The change law of burst failure release projectile performance is consistent with the change law of dynamic expansion of failure boundary radius. The closer to the working face, the higher the burst risk. At a distance of 10 m from the working surface, the maximum principal stress reaches its maximum value. The butterfly-shaped failure system generated by the surrounding rock of the roadway has energy self-sustainability, and the elastic energy released by the sudden expansion of the butterfly leaf is enough to cause a burst damage of 1.9 magnitude.

Acknowledgements This research is financially supported by the National Natural Science Foundation of China (52004291, 52130409, 51874314), the Research Fund of State and Local Joint Engineering Laboratory for Gas Drainage & Ground Control of Deep Mines (Henan Polytechnic University) (SJF202003), the Fundamental Research Funds for the Central Universities (2022XJAJQ02), the Innovative Training Program for College Students (C202112035, C202112003).

Author Contribution Feng Du: Methodology, Investigation, Writing-original draft. Ji Ma: Formal analysis, Investigation, Writing-original draft, Supervision. Xiaofei Guo: Formal analysis, Writing-review & editing. Tianfeng Wang: Investigation, Formal analysis. Xiaohang Dong: Conceptualization. Jiashuo Li: Formal analysis. Shulei He: Conceptualization, Formal analysis. Dilinaer Nuerjuma: Formal analysis.

Data Availability The data used to support the findings of this study are available from the corresponding author upon request.

Declarations

Declaration of competing interest The authors declare that they have no known competing financial interests or personal relationships that could have appeared to influence the work reported in this paper.

Open Access This article is licensed under a Creative Commons Attribution 4.0 International License, which permits use, sharing, adaptation, distribution and reproduction in any medium or format, as long as you give appropriate credit to the original author(s) and the source, provide a link to the Creative Commons licence, and indicate if changes were made. The images or other third party material in this article are included in the article's Creative Commons licence, unless indicated otherwise in a credit line to the material. If material is not included in the article's Creative Commons licence and your intended use is not permitted by statutory regulation or exceeds the permitted use, you will need to obtain permission directly from the copyright holder. To view a copy of this licence, visit <http://creativecommons.org/licenses/by/4.0/>.

References

- Bieniawski ZT, Denkhaus HG, Vogler UW (1969) Failure of fractured rock. *Int J Rock Mech Min Sci Geomech Abstracts* 6(3):323–330 IN29-IN32
- Chen B (2020) Stress-induced trend: the clustering feature of coal mine disasters and earthquakes in China. *Int J Coal Sci Technol* 7(3625):676–692
- Dai L, Pan Y, Li Z, Wang A (2021) Quantitative mechanism of roadway rockbursts in deep extra-thick coal seams: Theory and case histories. *Tunn Undergr Space Technol* 111:103861
- Du F, Wang K (2019) Unstable failure of gas-bearing coal-rock combination bodies: Insights from physical experiments and numerical simulations. *Process Saf Environ Prot* 129:264–279
- Du F, Wang K, Zhang X, Xin C, Wang G (2020) Experimental Study of Coal-Gas Outburst: Insights from Coal-Rock Structure, Gas Pressure and Adsorptivity. *Nat Resour Res* 29(4):1–13
- Fan CJ, Li S, Luo Mk, Du WZ, Yang ZH (2017) Coal and gas outburst dynamic system. *Int J Min Sci Technol* 27(1):49–55
- Hao Z (2018) Evolution Law of Plastic Zone and Burst Failure Mechanism of Gateway in Yima Coalfield. China University of mining and technology, Beijing, Beijing
- He S, Song D, Mitri H, He X, Chen T (2021) Integrated rockburst early warning model based on fuzzy comprehensive evaluation method. *Int J Rock Mech Min Sci* 142(4):104767
- Jiang L, Kong P, Zhang P, Shu J, Wu Q (2020) Dynamic Analysis of the Rock Burst Potential of a Longwall Panel Intersecting with a Fault. *Rock Mech Rock Eng* 53(4):1737–1754
- Jiang Y, Pan Y, Jiang F (2014) State of the art review on mechanism and prevention of coal bumps in China. *J China Coal Soc* 39(2):205–213
- Jiao Z (2017) Research on the evolution law of fault slip and mechanism of coal bumps induced by mining. China University of Mining & Technology, Beijing, Beijing
- Konicek P, Waclawik P (2018) Stress changes and seismicity monitoring of hard coal longwall mining in high rockburst risk areas. *Tunn Undergr Space Technol* 81:237–251
- Li Q (2021) The view of technological innovation in coal industry under the vision of carbon neutralization. *Int J Coal Sci Technol* 8:1197–1207
- Li X et al (2016) Rock Burst Monitoring by Integrated Microseismic and Electromagnetic Radiation Methods. *Rock Mech Rock Eng* 49(11):4393–4406
- Li X et al (2017) Failure mechanism and coupled static-dynamic loading theory in deep hard rock mining: A review. *J Rock Mech Geotech Eng* 9(4):767–782
- Li XL, Chen SJ, Li ZH, Wang EY (2021) Rockburst mechanism in coal rock with structural surface and the microseismic (MS) and electromagnetic radiation (EMR) response. *Eng Fail Anal* 124(6):105396
- Li ZL, He XQ, Dou LM, Song DZ, Wang GF (2018) Numerical investigation of load shedding and rockburst reduction effects of top-coal caving mining in thick coal seams. *Int J Rock Mech Min Sci* 110:266–278
- Ma N, Guo X, Zhao Z, Zhao X (2016) Occurrence mechanisms and judging criterion on circular tunnel butterfly rock burst in homogeneous medium. *J China Coal Soc* 41(11):2679–2688
- Ma J, Zhao Z, Haoyu S, Guo X (2019a) Sources of seismic energy based on butterfly failure theory. *J China Coal Soc* 44(6):1654–1665
- Ma N, Ma J, Zhao Z, Guo X (2019b) Mechanical mechanism and evolution of X-shaped conjugate shear fractureseism. *J China Coal Soc* 44(6):1647–1653
- Pan Y (2018) Disturbance response instability theory of rockburst in coal mine. *J China Coal Soc* 43(8):2091–2098
- Qi Q, Li X, Zhao S (2013) Theory and Practices on Stress Control of Mine Pressure Bumping. *Coal Sci Technol* 6(41):1–5
- Qi Q, Li Y, Zhao S (2019) Discussion on the mechanism and control of coal bump among mine group. *J China Coal Soc* 44(1):141–150
- Salamon MDGR (1990) Mechanism of caving in longwall mining, Rock Mechanics Contributions and Challenges: Proc 31st US Symposium, Golden

- Si L, Wei J, Xi Y, Wang H, Zhang H (2021) The influence of long-time water intrusion on the mineral and pore structure of coal. *Fuel* 290(1):119848
- Wang GF, Gong SY, Dou LM, Cai W, Yuan XY, Fan CJ (2019) Rockburst mechanism and control in coal seam with both syncline and hard strata. *Saf Sci* 115:320–328
- Wang K, Du F (2020) Coal-gas compound dynamic disasters in China: A review. *Process Saf Environ Prot* 133:1–17
- Yardimci AG, Karakus M (2020) A new protective destressing technique in underground hard coal mining. *Int J Rock Mech Min Sci* 130:10432
- Yuan L (2016) Control of coal and gas outbursts in Huainan mines in China: A review. *J Rock Mech Geotech Eng* 4(8):559–567
- Zhang J, Jiang F, Yang J, Bai W, Zhang L (2017) Rockburst mechanism in soft coal seam within deep coal mines. *Int J Min Sci Technol* 27(3):551–556
- Zhang M (1987) Instability Theory and Mathematical Model for Coal/rock bursts. *J China Coal Soc* 3(6):197–204
- Zhao Y, Zhou J, Wengang L (2020) Characteristics of ground pressure and mechanism of coal burst in the gob side roadway at Xinjie deep mining area. *J China Coal Soc* 45(5):1595–1606
- Zhao Z et al (2013) Partitioning characteristics of gas channel of coal-rock mass in mining space and gas orientation method. *Int J Min Sci Technol* 23(6):873–877
- Zhou CY, Zhu FX (2010) An elasto-plastic damage constitutive model with double yield surfaces for saturated soft rock. *Int J Rock Mech Min Sci* 47(3):385–395
- Zhou J, Li X, Mitri HS (2018) Evaluation Method of Rockburst: State-of-the-art Literature Review. *Tunn Undergr Space Technol* 81:632–659
- Zhu S, Yu F, Jiang F, Liu J (2018) Mechanism and risk assessment of overall-instability-induced rockbursts in deep island longwall panels. *Int J Rock Mech Min Sci* 106:342–349

Publisher's Note Springer Nature remains neutral with regard to jurisdictional claims in published maps and institutional affiliations.